



## Technical Note

## Effects of the upper inflow area on pool boiling heat transfer in a vertical annulus

Myeong-Gie Kang\*

Department of Mechanical Engineering Education, Andong National University, 388 Songchun-dong, Andong-city, Kyungbuk 760-749, South Korea

## ARTICLE INFO

## Article history:

Received 2 October 2008  
 Received in revised form 2 April 2009  
 Accepted 2 April 2009  
 Available online 6 June 2009

## Keywords:

Pool boiling  
 Heat transfer  
 Annulus  
 Flow area  
 Vertical tube

## ABSTRACT

The upper inflow area has been changed to identify the effects of it on pool boiling heat transfer in a vertical annulus. Both bottom inflow conditions of the open and the closed are considered for the study. For the test, a heated tube of 25.4 mm diameter and the water at atmospheric pressure have been used. The ratios of the gaps have been varied from 0.18 to 1. Effects of the inflow area on heat transfer become evident as the heat flux increases and the gap ratio decreases. If the gap ratio is smaller than 0.51 and the heat flux is higher than 60 kW/m<sup>2</sup>, a noticeable decrease in heat transfer is observed. The major cause for the tendency is attributed to the formation of a lumped bubble around the upper regions of the annulus.

© 2009 Elsevier Ltd. All rights reserved.

## 1. Introduction

The mechanism of pool boiling heat transfer has been studied extensively for the several decades [1]. Although many workers have investigated effects of heater geometries on boiling heat transfer, knowledge on the confined spaces on pool boiling heat transfer is still limited. Studies on the crevices can be divided into two categories. One of them is about annuli [2–5] and the other one is about plates [6–8]. In addition to the geometric conditions, flow to the crevices can be controlled. Some geometry has a closed bottom [2,5,6].

It is well known from the literature that the confined boiling is an effective technique to enhance heat transfer. It can result in heat transfer improvements up to 300–800% at low heat fluxes, as compared with unconfined boiling [2,6]. However, a sudden deterioration of heat transfer appears at high heat fluxes for confined boiling [6,8]. The boiling heat transfer coefficient usually increases when the gap size decreases at low heat fluxes whereas it decreases at higher heat fluxes. However, in general, the heat transfer coefficient increases when the gap size decreases to a certain value [2–4,7] at low heat fluxes. Further decrease in the gap size results in a sudden decrease of the heat transfer coefficient. One of the possible reasons of the deterioration is a formation of big bubbles followed after active bubble coalescence at the upper regions of the annulus [4].

Around the upper region of the annulus with a closed bottom the downward liquid flow interferes with the upward bubble flow. Thereafter, bubbles are coalescing to a big lump while fluctuating

up and down in the annular gap. Kang [5] published effective results of moving the deterioration point, where a sudden decrease in heat transfer was observed comparing to the unrestricted single tube, to the higher heat flux and of preventing the occurrence of the critical heat flux. To remove the coalescence of the big bubbles around the upper region of the annulus Kang [5] controlled the length of the outer tube of the annulus. The major cause of the big bubble formation which results in the deterioration is partly because of the no inflow through the lower regions of the annulus. Kang [9] identifies that the inflow area at the bottom regions of an annulus changes heat transfer coefficients much and moves the deterioration point of the heat transfer coefficients to the higher heat fluxes.

Summarizing the previous works about the pool boiling heat transfer in an annulus, it can be stated that heat transfer coefficients are highly dependent on the geometry and the confinement condition. One of the interesting and important geometric parameters in pool boiling heat transfer is the inflow area at the upside region of the annulus. The variation of the upper inflow area changes the outward velocity of the bubbles from the annulus. This kind of geometry is found in an in-pile test section that is important to identify nuclear fuel irradiation behavior at the operating condition of a commercial power plant. Up to the author's knowledge, no previous results concerning to this effect have been published yet. Therefore, the results of this study could provide a clue to the thermal design of those facilities.

## 2. Experiments

A schematic view of the present experimental apparatus and a test section is shown in Fig. 1. The water tank (Fig. 1(a)) is made

\* Tel.: +82 54 820 5483; fax: +82 54 823 1766.  
 E-mail address: [mgekang@andong.ac.kr](mailto:mgekang@andong.ac.kr).

### Nomenclature

$A_T$	data acquisition error, °C	$q''$	heat flux, W/m <sup>2</sup>
$D$	diameter of the heating tube, m	$s$	gap size ( $= (D_i - D)/2$ ), m
$D_i$	inside diameter of the glass tube, m	$s_d$	gap size around the flow interrupter ( $= (D_i - d)/2$ ), m
$d$	diameter of the flow interrupter, m	$s_r$	ratio of the gaps ( $= s_d/s$ )
$h_b$	boiling heat transfer coefficient, W/m <sup>2</sup> ·°C	$T_{sat}$	saturation temperature, °C
$I$	supplied current, A	$T_W$	tube wall temperature, °C
$L$	heated tube length, m	$V$	supplied voltage, V
$P_T$	precision limit, °C	$\Delta T_{sat}$	tube wall superheat ( $= T_W - T_{sat}$ ), °C

of stainless steel and has a rectangular cross section (950 × 1300 mm) and a height of 1400 mm. The sizes of the inner tank are 800 × 1000 × 1100 mm (depth × width × height). Four auxiliary heaters (5 kW/heater) are installed at the space between the inside and the outside tank bottoms. The heat exchanging tube is a resistance heater (Fig. 1(b)) made of a very smooth stainless steel tube ( $L = 0.5$  m and  $D = 25.4$  mm). The surface of the tube is finished through a buffing process to have a smooth surface. Electric power of 220 V AC is supplied through the bottom side of the tube.

The tube outside is instrumented with five T-type sheathed thermocouples (diameter is 1.5 mm). The thermocouple tip (about 10 mm) is brazed on the tube wall. The brazing metal is a kind of brass and the averaged brazing thickness is less than 0.1 mm. The temperature decrease along the brazing metal is calibrated by the one dimensional conduction equation. The water temperatures are measured with six sheathed T-type thermocouples brazed on a stainless steel tube that placed vertically at a corner of the inside tank. All thermocouples are calibrated at a saturation value (100 °C since all tests are done at atmospheric pressure). To measure and/or control the supplied voltage and current, two power supply systems are used.

For the tests, the heat exchanging tube is assembled vertically at the supporter (Fig. 1(a)) and an auxiliary supporter is used to fix a glass tube (Fig. 1(b)). To make the annular condition, a glass tube of 55.4 mm inner diameter ( $D_i$ ) and 600 mm length are situated around the heated tube. The gap size ( $s = (D_i - D)/2$ ) of the main body of the annulus is 15 mm. A glass tube without the bottom inflow holes is used for the test of the bottom closed annulus. To maintain the gap size between the heated tube and the glass tube a spacer (Fig. 2(b)) has been installed at the upper region of the test section. The upper inflow into the annular space is controlled by the flow interrupters (Fig. 2(c)) that having the outside diameters ( $d$ ) of 40, 45, and 50 mm, respectively. After installing the flow interrupter around the test section the spacer is screwed down on the test section tightly. Because of the flow interrupter the gap size around the interrupter ( $s_d = (D_i - d)/2$ ) is different from the gap of the main body. The ratio of the gaps ( $s_r = s_d/s$ ) varies from 0.18 to 1 as shown in Table 1. Among the values  $s_r = 1$  represents the annulus without the flow interrupter.

After the water tank is filled with water until the initial water level gets 1100 mm, the water is then heated using four pre-heaters at constant power. When the water temperature is reached at the saturation value, the water is then boiled for 30 minutes to

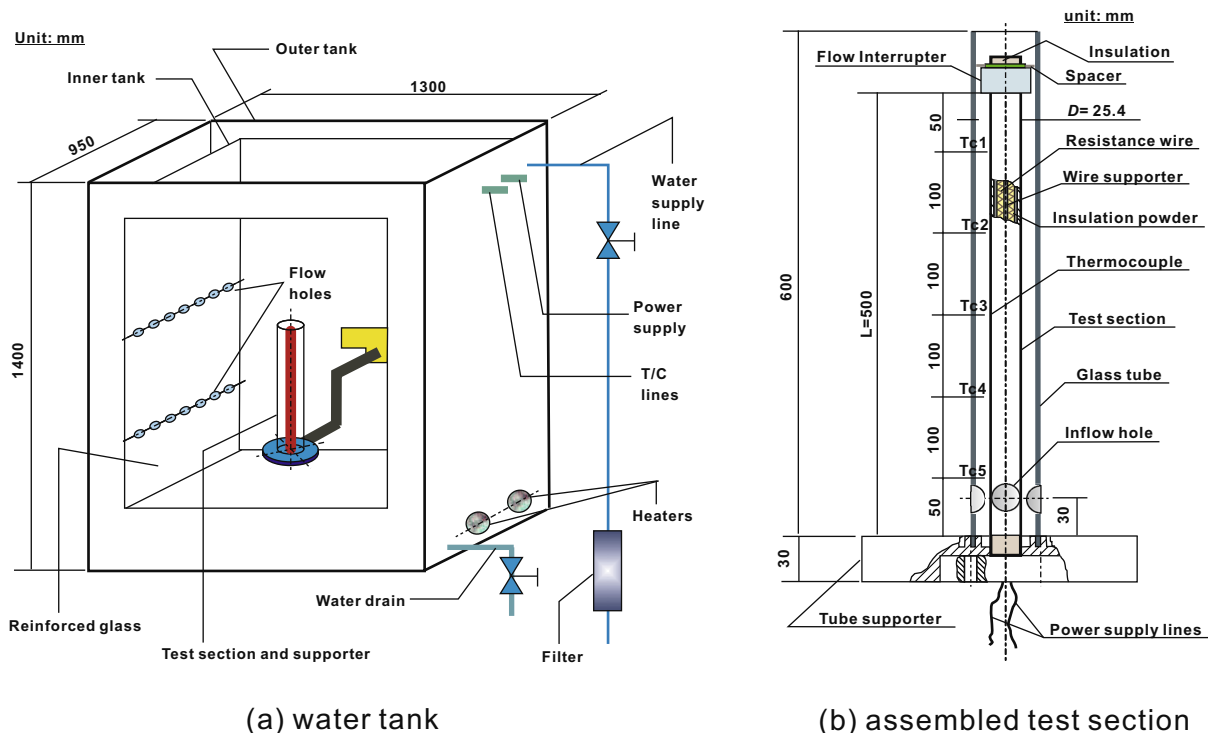


Fig. 1. Schematic of the experimental apparatus.

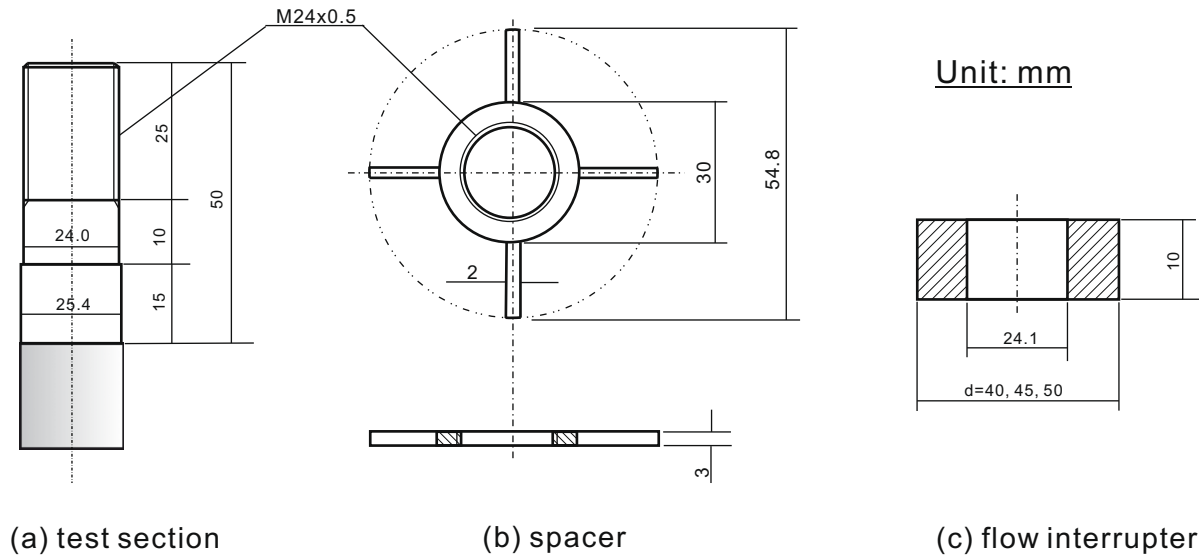


Fig. 2. Detailed views of the test tube upper regions.

Table 1  
Test matrix and  $q''$  versus  $\Delta T_{sat}$  data.

$d$ (mm)	$s_d$ (mm)	$s_r$ ( $s_d/s$ )	$q''$ (kW/m <sup>2</sup> )	Remark	Number of data
–	–	–	0–120	Single	12
–	15.0	1	0–120	Bottom open	12
40	7.7	0.51	0–120	Bottom open	12
45	5.2	0.35	0–120	Bottom open	12
50	2.7	0.18	0–120	Bottom open	12
–	15.0	1	0–120	Bottom closed	12
40	7.7	0.51	0–120	Bottom closed	12
45	5.2	0.35	0–120	Bottom closed	12
50	2.7	0.18	0–120	Bottom closed	12

remove the dissolved air. The temperatures of the tube surfaces ( $T_W$ ) are measured when they are at steady state while controlling the heat flux on the tube surface with input power.

The heat flux from the electrically heated tube surface is calculated from the measured values of the input power as follows:

$$q'' = \frac{VI}{\pi DL} = h_b \Delta T_{sat} = h_b (T_W - T_{sat}) \quad (1)$$

where  $V$  and  $I$  are the supplied voltage and current, and  $D$  and  $L$  are the outside diameter and the length of the heated tube, respectively.  $T_W$  and  $T_{sat}$  represent the measured temperatures of the tube surface and the saturated water, respectively. Every temperature used in Eq. (1) is the arithmetic average value of the temperatures measured by the thermocouples.

The uncertainties of the experimental data are calculated from the law of error propagation [10]. The data acquisition error ( $A_T \pm 0.05$  °C) and the precision limit ( $P_T \pm 0.1$  °C) have been counted for the uncertainty analysis of the temperature. The 95% confidence uncertainty of the measured temperature is calculated from  $(A_T^2 + P_T^2)^{1/2}$  and has the value of  $\pm 0.11$  °C. The error bound of the voltage and current meters used for the test is  $\pm 0.5\%$  of the measured value. Therefore, the uncertainty of the calculated power (voltage  $\times$  current) has been obtained as  $\pm 0.7\%$ . Since the heat flux has the same error bound as the power, the uncertainty in the heat flux is estimated to be  $\pm 0.7\%$ . When evaluating the uncertainty of the heat flux, the error of the heat transfer area is not counted since the uncertainty of the tube diameter and the length is  $\pm 0.1$  mm and its effect on the area is negligible. To determine the uncertainty of the heat transfer coefficient the uncertainty propagation equation

has been applied on the Eq. (1). Since values of the heat transfer coefficient are resulted from the calculation of  $q''/\Delta T_{sat}$  a statistical analysis on the results has been performed. After calculation and taking the mean of the uncertainties of the propagation errors the uncertainty of the heat transfer coefficient can be decided as  $\pm 6\%$ .

### 3. Results and discussion

Fig. 3 shows variations in heat transfer as the diameter of the flow interrupter changes. Because of the interrupter the heat transfer rate gets deteriorated comparing to the rate for the annulus without the interrupter. For a given flow interrupter, the effect of the gap ratio on heat transfer is slightly greater for the open than the closed bottom. For example,  $\Delta T_{sat}$  increases only 8.7% (from 4.6 to 5 °C) when  $s_r$  is decreased by 82% (from 1 to 0.18) at the given heat flux ( $q'' = 120$  kW/m<sup>2</sup>). For the annulus with an open bottom, on the other hand, Fig. 3(a) shows that the effect of the interrupter on heat transfer is remarkably bigger than that for the closed bottom. According to Fig. 3(a),  $\Delta T_{sat}$  increases more than 20.8% (from 4.8 to 5.8 °C) under the same conditions used for the closed bottom. The slope of  $q''$  versus  $\Delta T_{sat}$  curve of the bottom open becomes smaller than that of the bottom closed annulus as the gap ratio decreases from  $s_r = 1$  to  $s_r = 0.18$  and  $q'' > 60$  kW/m<sup>2</sup>.

In general, as shown in Fig. 3(a), the heat transfer rates for the annuli with open bottoms are higher than the single unrestricted tube. When the heat flux is higher than 60 kW/m<sup>2</sup> and the gap ratio is equal to 0.18, the heat transfer for the annulus gets decreased than that of the single tube. When the gap ratio is  $s_r = 0.18$ , the slopes of  $q''$  versus  $\Delta T_{sat}$  curve shown in Fig. 3(a) shifts and crosses the curve of the single unrestricted tube at about  $\Delta T_{sat} = 4.7$  °C and  $q'' = 60$  kW/m<sup>2</sup>. For the heat fluxes smaller than 60 kW/m<sup>2</sup> the heat transfer rate for the annulus is greater than the single tube regardless of the gap ratio. As the boiling becomes more vigorous, especially for the small gap ratios, the heat transfer for the annulus gets decreased comparing to the single tube.

The rate of heat transfer for the annulus with a closed bottom, Fig. 3(b), is higher than the single unrestricted tube throughout the tested heat fluxes. The characteristic of heat transfer can be divided into two categories according to the heat flux. For the heat fluxes lower than 60 kW/m<sup>2</sup> heat transfer for the annuli is much greater than the single tube and has similar curve slopes comparing

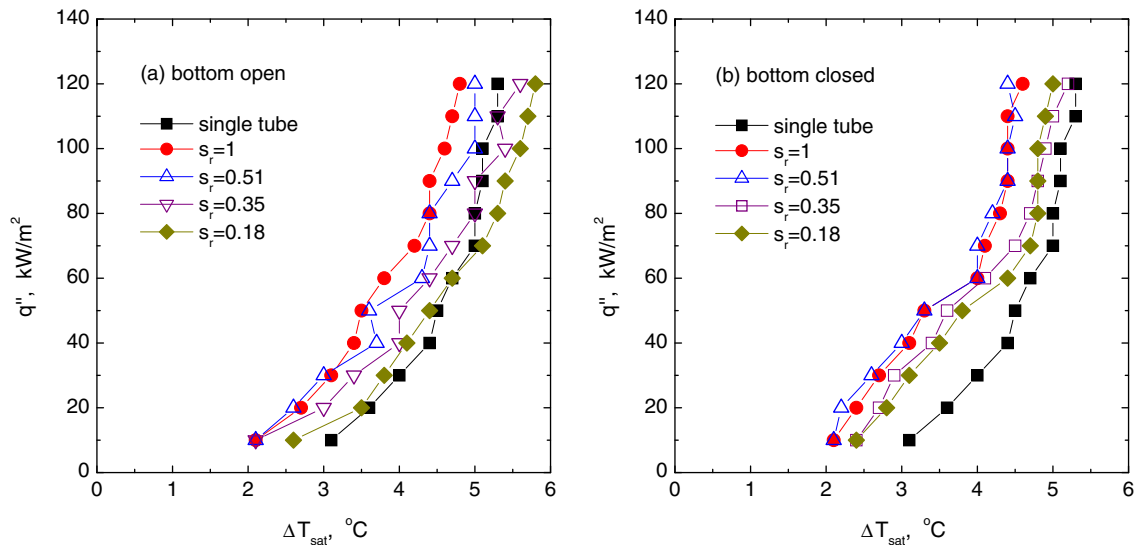


Fig. 3. Plots of  $q''$  versus  $\Delta T_{sat}$  for the different flow interrupter and the annulus condition.

to the curve of the annulus without the flow interrupter. When  $s_r \leq 0.35$  and the heat flux increases more than  $60 \text{ kW/m}^2$  the curves with the flow interrupter are seen to merge into the curve of the single unrestricted tube. Along the heat fluxes the slope of the curve for  $s_r = 0.51$  is similar to that of the annulus without the interrupter.

In summary, Fig. 3(a) and (b) show that the flow interrupters deteriorate heat transfer. The reason for this may be attributable to the following phenomena:

- (1) The flow interrupter obstructs the outward bubble flow from the annulus with an open bottom. Because of the interrupter a kind of bottleneck is created just below the interrupter. Then, the detached bubbles coming from the lower part of the tube get stagnant for a while and accumulate at the upper region of the annulus. During the stay the bubbles are coalescing together and are growing to a big lump of bubble. Thereafter, the upward rising velocity of the fluid gets decreased because of the lump. Since the major heat transfer resistance is the heat conduction across the liquid film, the reduced film thickness under the bubbles increases the heat transfer coefficient [3]. When the fluid velocity decreases the shear stress on the liquid film at the heated surface decreases and, accordingly, the thickness of the liquid film gets increased. The thickened film decreases heat transfer. The tendency of decreasing heat transfer due to the decrease in the fluid velocity is also observed in the forced convective nucleate boiling [11]. The size of the bubble lump is increasing until the amount of the buoyancy is enough to escape from the gap space. The increase in the heat flux leads to the decrease in the heat transfer rate since more bubbles are generated on the tube surface.
- (2) For the annulus with a closed bottom, more complicated bubble movement and liquid mixing is observed than the open bottom. The environment liquid should enter through the upper side of the annulus while the bubbles are flowing out. Because of the countercurrent flow a serious interference is generated between the outward bubbles and the incoming liquid. The interference is caused because of the friction force generated between the flows. This friction, then, disturbs the outward bubble flow and creates big lumps of bubbles in the annular space. The lumps get stag-

nant and coalesce with other bubbles in a consequence of the obstruction. The smaller the gap ratio the bigger the bubbles will be. Since there is no inflow from the lower part of the annulus, the size of the lump of bubble increases much bigger than the lumps observed in the annulus with an open bottom. If the lump flows out a vacancy is created in the gap space. Then, a sudden rush of the liquid is occurred. During the process the inside fluid is accelerated to move up and downward, generating a pulsating flow, in the gap space. As a result very active liquid agitation is observed visually. The high rate of heat transfer by boiling in the gap space has been ascribed to the intense agitation of the liquid at the heating surface by the bubbles [11]. The generation of the big size bubble lumps resulted in the decrease in the intensity of liquid agitation. If big size bubble lumps were generated, the intensity of the liquid agitation should be decreased since the length for the flow acceleration is shortened. Moreover, the lumps prevent the smooth supply of liquid into the gap space. Thereafter the decrease in the heat transfer rate is caused. As the heat flux increases more bubbles are generated and these bubbles are coalescing together to create larger size bubbles in the gap space. If there is an enough flow area around the upper region of the annulus, the lumped bubbles agitate inside fluid while flowing outward without suffering a notable interference between the bubbles and the liquid. But, if the upper inflow area is not enough like the present study, the flow friction increases. The decrease in the heat transfer rate is accelerated as the value of the gap ratio decreases.

Fig. 4 shows some photos of pool boiling. Those photos are taken at around the mid-point of the tube length. The photos of the annuli are showing big bubbles inside the gap space comparing to the single unrestricted tube. For the annulus with an open bottom, the increase in the number and size of the bubbles are clearly observed in the gap space when the value of the gap ratio changes from  $s_r = 1$  to  $s_r = 0.18$ . The photos for the annulus with a closed bottom show no remarkable differences comparing to each other. Although not shown in the figure, the visual observation of the boiling phenomena indicates that, as the gap ratio decreases, more frequent generation of the bubble lumps is observed at the upper region of the annulus. This is accelerated as the heat flux increases.

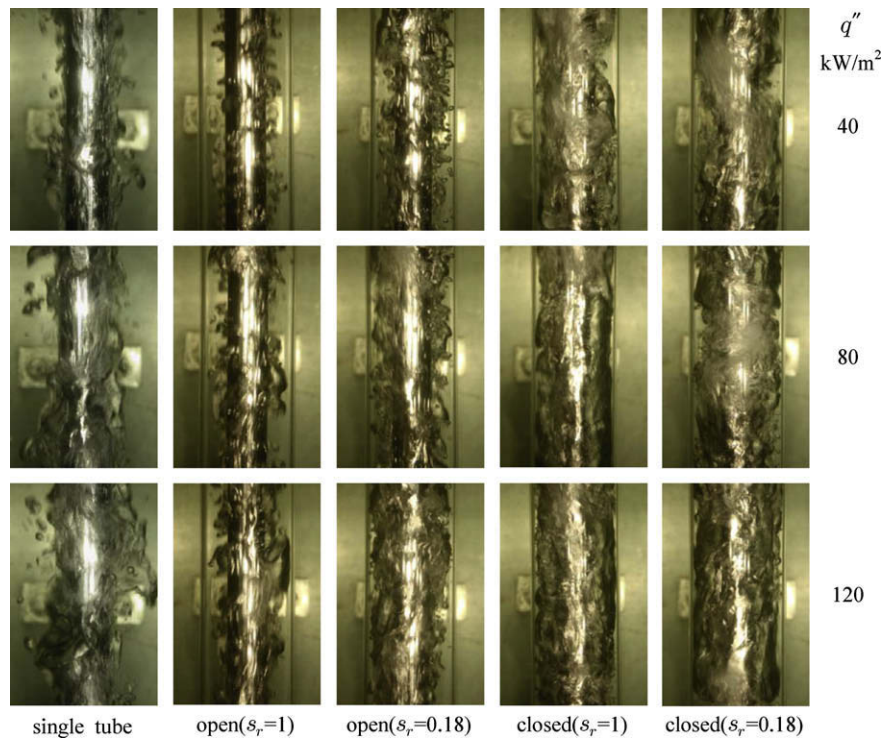


Fig. 4. Photos of pool boiling as the geometric condition and heat flux change.

#### 4. Conclusions

To investigate effects of the upside inflow area on pool boiling heat transfer in a vertical annulus, the gap size at the upper region of the annulus has been regulated from 2.7 to 15 mm using a flow interrupter. For the test, a heated tube of 25.4 mm diameter and the water at atmospheric pressure have been used. Major conclusions of the study are as follows:

- (1) Variation of the upside inflow area changes the tendency of heat transfer. As  $s_r \leq 0.35$  and  $q'' \geq 60 \text{ kW/m}^2$ , heat transfer gets deteriorated and the resulting curves merge to (for the closed bottom) or cross over (for the open bottom) the curve of the single unrestricted tube.
- (2) The causes of the heat transfer deterioration are recognized as the reduced liquid velocity and the decrease in liquid agitation for the annuli with open and closed bottoms, respectively.

#### References

- [1] M. Shoji, Studies of boiling chaos: a review, *Int. J. Heat Mass Transfer* 47 (2004) 1105–1128.
- [2] S.C. Yao, Y. Chang, Pool boiling heat transfer in a confined space, *Int. J. Heat Mass Transfer* 26 (1983) 841–848.
- [3] Y.H. Hung, S.C. Yao, Pool boiling heat transfer in narrow horizontal annular crevices, *ASME J. Heat Transfer* 107 (1985) 656–662.
- [4] M.G. Kang, Y.H. Han, Effects of annular crevices on pool boiling heat transfer, *Nucl. Eng. Des.* 213 (2002) 259–271.
- [5] M.G. Kang, Pool boiling heat transfer on a vertical tube with a partial annulus of closed bottoms, *Int. J. Heat Mass Transfer* 50 (2007) 423–432.
- [6] J. Bonjour, M. Lallemand, Flow patterns during boiling in a narrow space between two vertical surfaces, *Int. J. Multiphase Flow* 24 (1998) 947–960.
- [7] Y. Fujita, H. Ohta, S. Uchida, K. Nishikawa, Nucleate boiling heat transfer and critical heat flux in narrow space between rectangular spaces, *Int. J. Heat Mass Transfer* 31 (1988) 229–239.
- [8] J.C. Passos, F.R. Hirata, L.F.B. Possamai, M. Balsamo, M. Misale, Confined boiling of FC72 and FC87 on a downward facing heating copper disk, *Int. J. Heat Fluid Flow* 25 (2004) 313–319.
- [9] M.G. Kang, Pool boiling heat transfer in a vertical annulus as the bottom inflow area changes, *Int. J. Heat Mass Transfer* 51 (2008) 3369–3377.
- [10] H.W. Coleman, W.G. Steele, *Experimentation and Uncertainty Analysis for Engineers*, second ed., John Wiley & Sons, 1999.
- [11] W.M. Rohsenow, A method of correlating heat-transfer data for surface boiling of liquids, *ASME J. Heat Transfer* 74 (1952) 969–976.